Journal of Biotechnology 213 (2015) 28–41

Contents lists available at ScienceDirect

Journal of Biotechnology

journal homepage: www.elsevier.com/locate/jbiotec

Very high cell density perfusion of CHO cells anchored in a non-woven matrix-based bioreactor

Ye Zhang [a], Per Stobbe [b], Christian Orrego Silvander [c], Véronique Chotteau [a,*]

[a] School of Biotechnology, Dept. Industrial Biotechnology/Bioprocess Design, Cell Technology Group (CETEG), Royal Institute of Technology, KTH, SE-10691 Stockholm, Sweden
[b] PerfuseCell, Malmmosevej 19C, DK-2840 Holte, Denmark
[c] Belach Bioteknik, Dumpervägen 8, SE-14250 Skogås, Sweden[1]

ARTICLE INFO

Article history:
Received 22 October 2014
Received in revised form 10 July 2015
Accepted 14 July 2015
Available online 23 July 2015

Keywords:
Disposable bioreactor
On-line biomass sensor
IgG production
Dielectric spectroscopy
Hypothermia

ABSTRACT

Recombinant Chinese Hamster Ovary (CHO) cells producing IgG monoclonal antibody were cultivated in a novel perfusion culture system CellTank, integrating the bioreactor and the cell retention function. In this system, the cells were harbored in a non-woven polyester matrix perfused by the culture medium and immersed in a reservoir. Although adapted to suspension, the CHO cells stayed entrapped in the matrix. The cell-free medium was efficiently circulated from the reservoir into- and through the matrix by a centrifugal pump placed at the bottom of the bioreactor resulting in highly homogenous concentrations of the nutrients and metabolites in the whole system as confirmed by measurements from different sampling locations. A real-time biomass sensor using the dielectric properties of living cells was used to measure the cell density. The performances of the CellTank were studied in three perfusion runs. A very high cell density measured as 200 pF/cm (where 1 pF/cm is equivalent to 1×10^6 viable cells/mL) was achieved at a perfusion rate of 10 reactor volumes per day (RV/day) in the first run. In the second run, the effect of cell growth arrest by hypothermia at temperatures lowered gradually from 37 °C to 29 °C was studied during 13 days at cell densities above 100 pF/cm. Finally a production run was performed at high cell densities, where a temperature shift to 31 °C was applied at cell density 100 pF/cm during a production period of 14 days in minimized feeding conditions. The IgG concentrations were comparable in the matrix and in the harvest line in all the runs, indicating no retention of the product of interest. The cell specific productivity was comparable or higher than in Erlenmeyer flask batch culture. During the production run, the final harvested IgG production was 35 times higher in the CellTank compared to a repeated batch culture in the same vessel volume during the same time period.

1. Introduction

Perfusion bioprocesses have several advantages compared with batch/fed-batch processes such as a potential high cell density, a high productivity in a relatively small size bioreactor, a stable cell environment and long-term production (Castilho and Medronho, 2002; Chotteau, 2015; Chu and Robinson, 2001; Langer, 2011; Voisard et al., 2003).

Perfusion processes have become increasingly accepted in the past decade for the commercial manufacturing of biopharmaceuticals due to, on one hand, the increasing use of disposable bioreactor systems alleviating the technical and sterility challenges, the need of flexibility and smaller equipment footprint for manufacturing, and, on the other hand, the emergence of robust perfusion systems, e.g., the alternating tangential flow filtration (Clincke et al., 2013a,b). Another field of application of perfusion processes is the production of biologics as research tools where given amounts of protein products are needed within a very short time period. For this kind of application, quite often neither the cell line nor the process/cultivation medium is optimized. High cell densities potentially provided by the perfusion mode can advantageously compensate for these sub-optimal conditions. Furthermore, perfusion mode offers a stable and continuously renewed cell environment favorable for the control of the product quality and can be necessary in the case of labile proteins.

Abbreviations: CHO, Chinese Hamster Ovary; CSPR, cell specific perfusion rate; DO, dissolved oxygen; HPLC, high-performance liquid chromatography; LDH, lactate dehydrogenase; RV/day, reactor volume per day.

* Corresponding author.
E-mail addresses: yezhang@kth.se (Y. Zhang), chotteau@kth.se (V. Chotteau).

[1] Presently Serendipity Innovations, Stureplan 15, SE-11145 Stockholm, Sweden.

http://dx.doi.org/10.1016/j.jbiotec.2015.07.006

In perfusion mode the cells are retained inside the bioreactor by anchoring them to a support, i.e., membrane, matrix, etc., (Meuwly et al., 2007) or by a cell retention device (Kompala and Ozturk, 2005). The former often applies to anchorage-dependent cells and the latter to suspension cell lines for which various commercial cell retention systems are available, based on e.g., filtration, acceleration. Several commercial systems based on anchoring the cells are available such as packed-bed with immobilized microcarriers (Bohak et al., 1987; Looby and Griffiths, 1988), ceramics matrix (Mitsuda et al., 1991), hollow fiber bioreactors (Knazek et al., 1972). Other techniques where the cells are entrapped in large polymer matrix have also been proposed: Lee et al. (2005) have developed a system in which the cells are entrapped in a depth filter, through which the medium is circulated by a peristaltic pump to a second tank equipped with monitoring and control systems. In a typical fibrous bioreactor, the cells are anchored in a fibrous matrix immersed in a tank and homogenized by magnetic stirring (Chen et al., 2002). In such bioreactor systems, gradients of the nutrients, gas composition, accumulation of dead cells in the supporting matrices and by-products heterogeneous distribution have often been reported, see for instance de la Broise's or Piret's reports (de la Broise et al., 1992; Piret and Cooney, 1990). These gradients are sub-optimal since they may cause a non-homogeneous cell environment with variations of the concentrations of the nutrients and toxic by-products, as well as an uneven distribution of the cell population. These can cause differential production in terms of quantity and quality of the product, cell selection and even necrosis in extreme cases.

Oh and Chang (1992) achieved a density of 187×10^6 hybridoma cells/mL in a dual hollow fiber bioreactor and up to 38.1×10^6 Vero cells/mL (Choi et al., 1995) and 33.5×10^6 CHO cells/mL (Lee et al., 2005) were reported using depth filter perfusion systems. These cell densities were estimated from either the cell specific productivity (Lee et al., 2005; Oh and Chang, 1992) or specific metabolite production/consumption rates (Choi et al., 1995), postulating that these specific rates were constant, which could not be verified, leading to uncertainty: for instance, for the same experiment Oh et al. (1994) reported maximal densities of 3×10^7 and 6×10^7 cells/mL based on either the cell specific glucose consumption rate or the cell specific IgG production rate (q_{IgG}) using a depth filter perfusion system.

In bioreactors with immobilized cells, cell sampling is difficult or impossible to perform but bioimpedance sensing can be used to monitor the biomass. Bioimpedance or dielectric spectroscopy is widely used as online biomass monitoring of upstream processes for different cell types such as yeast, bacteria, insect, mammalian cells (Ansorge et al., 2007; Carvell and Dowd, 2006; Harris et al., 1987; Kaufmann et al., 1999; Sarra et al., 1996; Zeiser et al., 1999). The bioimpedance biomass sensor utilizes the dielectric properties of living cells with intact plasma membrane. Due to the fact that the cell plasma membranes are poor electrical conductor, the cells act as small capacitors in an electrical field with charge built up on the membranes (Kaufmann et al., 1999). Applying a periodically alternating electrical field to the cell culture, the lag in the system response, caused by the polarization of the cell membranes, is detected as capacitance/permittivity signal. This signal is a function of the frequency of the electrical field switch and depends of the characteristic of the cells but the contribution from the medium components, the dead cells, the cell debris, etc. is negligible. Bioimpedance has been proposed as a promising tool for process analytical technology (PAT) introduced by the FDA in 2004 (Clementschitsch and Bayer, 2006; Gnoth et al., 2007; Teixeira et al., 2009).

Lowering the culture temperature in perfusion cultivations to arrest the cell growth and enhance q_{IgG} has been reported by others (Ahn et al., 2008; Chen et al., 2004; Ducommun et al., 2002b; Rodriguez et al., 2010; Tsai et al., 1996) and offers a simple approach to maintain the cell density.

The bioreactor used in the present study, CellTank, is a new concept that has been developed to perfuse adherent or non-adherent mammalian cells at high density. It is a compact disposable system where the cells are entrapped in a non-woven polyester matrix caged in a cassette and immersed in a reservoir. The cultivation medium rapidly circulates continuously through the matrix pumped by a centrifugal pump integrated in the reservoir. The CellTank has some common features with e.g., the packed bed, the fibrous bioreactor or the hollow fiber bioreactor hence the cells are immobilized while the medium is circulated. However the bioreactor design and technology are quite different. The system can operate with suspension cells and has been designed to ensure a highly homogeneous distribution of the fluid in the matrix.

In the present study, CellTank bioreactors were used to cultivate a suspension CHO K1 cell line producing recombinant IgG. Three perfusion runs were performed aiming at evaluating the performance of the CellTank. The purpose of the first run was to investigate the capacity of the CellTank to support high cell densities. In the second run, the effect of hypothermia on the growth and production at high cell density was studied. A selected temperature switch was finally applied in the third culture at 100 pF/cm cell density, and the stability as well as reproducibility of the CellTank performances were examined.

2. Materials and methods

2.1. Cell line and media

CHO DP-12 clone #1934 (ATCC) cells producing an IgG monoclonal antibody were adapted to suspension and serum-free culture in animal component-free IS CHO CD XP medium with hydrolysate (Irvine Scientific, USA), supplemented with 4 mM L-glutamine. The cells were expanded in 250 mL or 500 mL Erlenmeyer flasks (100 rpm agitation, 37 °C, 5% CO_2). The medium for perfusion cultivation was IS CHO CD XP medium with hydrolysate, supplemented with 3% IS CHO FEED CD XP (Irvine Scientific, USA) and 0.1 mg/mL streptomycin/100 mL/U penicillin G/0.25 μg/mL amphotericin B (all Sigma–Aldrich, USA). Additional supplementations of 15–30 mM D-(+)-glucose (stock solution 45%, Sigma–Aldrich, USA) and 1–4 mM L-glutamine (stock solution 200 mM, Irvine Scientific, USA) were performed to compensate for the cell consumption.

2.2. Set-up and equipment

The cultivation runs were performed in e-beam irradiated CellTank prototypes manufactured at PerfuseCell (2 L total volume), containing a 150 cm^3 non-woven matrix cassette immersed in 1 L culture medium. The matrix was composed of spun polyester fibers with diameter 20 μm and pore size less than 0.5 mm. The pH, dissolved oxygen (DO) and temperature were monitored and controlled with a Biophantom process control system (Belach Bioteknik, Sweden). The cell biomass was monitored by an iBiomass EVO 200 system at frequencies 1000 kHz and 10 MHz (Fogale Nanotech, France), with sampling every 120 s. The cell concentration was based on the cassette volume of 150 mL and a reading of 1 pF/cm corresponded to 1×10^6 viable cells/mL, see Section 3.2 for details. A dummy biomass probe was pre-installed in the middle of the matrix during e-beam irradiation and was replaced by an autoclaved biomass probe installed inside a laminar flow cabinet. The probes of pH and DO (Broadley–James) were autoclaved and mounted in the reservoir. The pH (set-point 7.0) was controlled by automatic addition of Na_2CO_3 0.5 M or CO_2 into the reservoir

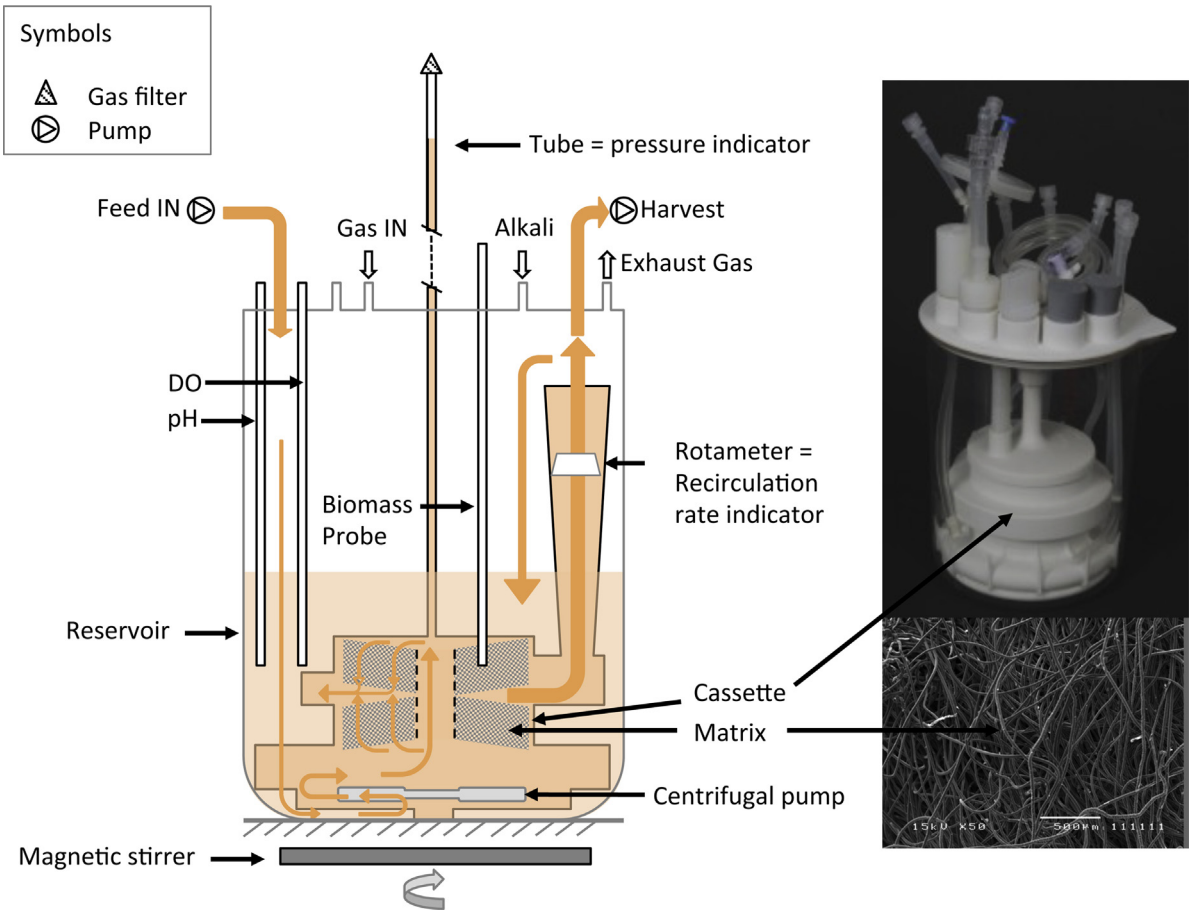

Fig. 1. Scheme of the CellTank perfusion culture system. Left: longitudinal section of the bioreactor. The arrows indicate the direction of fluid recirculation inside the bioreactor; Upper right: picture of the CellTank prototype; Lower right: enlargement of the matrix (50× magnification).
Picture courtesy of www.perfusecell.com.

headspace. The temperature sensor was mounted in a pouch plunging in the reservoir. The temperature was controlled using a heating blanket (100 W, 24 V) around the reservoir. The medium recirculation in the bioreactor was performed by an integrated centrifugal pump that was magnetically driven by a stirrer located under the bioreactor (two stirrer prototype systems were used manufactured by Belach and by PerfuseCell, respectively). The recirculation flow rate could be read on the rotameter (0.4–2.4 L/min) at the exit of the cassette and adjusted by varying the magnetic stirring speed of the centrifugal pump. A detailed sketch for the centrifugal pump is provided as Supplementary material. The medium perfusion was performed in the reservoir by two peristaltic pumps (Watson-Marlow 120U). The feed medium was prepared every day with glutamine and glucose additions calculated to compensate for the cell consumption. Fig. 1 illustrates the general set-up.

Supplementary material related to this article found, in the online version, at http://dx.doi.org/10.1016/j.jbiotec.2015.07.006

A continuous gas mix of air, N_2 and CO_2 was added into the headspace to steadily maintain a slight overpressure, ensuring the sterility of the system, and maintaining $pCO_2 > 2$ kPa. Due to the small culture volume (150 cm^3 matrix cassette), the DO was above the set point (40%) with only air addition at low or medium cell densities. Therefore air (0–100 mL/min) and N_2 (0–150 mL/min) were manually mixed at a concentration lower than 40% air. The DO was automatically controlled upwards by adding O_2 (0–60 mL/min) to the headspace or through a sparger in the reservoir. The sparger consisted of an obturated dip tube punctured with holes. The gas outlet was expelled via a 'bubble flask', i.e., a sterile flask half filled with water in which the outlet gas was bubbling. Pressure inside the cassette was measured by a tube vertically mounted on top of the matrix, see Fig. 1. The liquid level in this tube was a linear indicator of the pressure inside the matrix, i.e., similarly to a barometer.

2.3. Methods

The CellTank was inoculated from Erlenmeyer flask cultures in exponential growth phase at 1×10^6 viable cells/mL for run#1 and run#2 using the feed-in line into the reservoir and the recirculation flow rate was set to 1.0 L/min. Run#3 was seeded at 2×10^6 viable cells/mL. The perfusion was initiated when the cell reached 2 pF/cm in the matrix after growing them in batch mode. The recirculation flow rate was then maintained at 1.6 L/min until the end of the runs. Samples from the reservoir, the matrix (from a hole drilled in the matrix) and the harvest line were daily taken.

A cell specific perfusion rate (CSPR) of 0.05 nL/cell/day (or 1/20 nL/cell/day) based on the reactor volume of 150 mL, which is the volume of the cassette, was adopted (Clincke et al., 2013b). To implement this CSPR, a practical way to calculate the perfusion rate (unit = RV/day) as a function of the viable cell density (C_v) given in Eq. (1), was used.

$$\text{Perfusion rate} = \text{CSPR}\, C_v = 0.05 \quad C_v = \frac{C_v}{20} \tag{1}$$

Furthermore the perfusion rate was manually increased above the value given by Eq. (1) when the levels of ammonia or lactate exceeded 4.8 mM and 50 mM, respectively.

2.4. Analytical methods

2.4.1. Quantification methods

The density of the cells leaking from the matrix, i.e., present in the reservoir, the pH, pCO_2, pO_2, osmolality, concentrations of glucose, lactate, glutamine, glutamate and ammonia, were measured by Bioprofile FLEX (Nova Biomedical). The perfusion rate was calculated based on the matrix volume (150 cm^3) by weighting the feed medium and harvest bottles. The cell viability was determined by measuring the activity of lactate dehydrogenase (LDH) (cytotoxicity enzymatic assay, Promega) to determine the concentration of dead cells, C_{dead}, in the daily harvest samples. A standard curve of released LDH activity was made from lysing known numbers of cells. The viability was then calculated as

$$\frac{C_v \mathrm{vol}_{matrix} 100\%}{C_v \mathrm{vol}_{matrix} + C_{dead}(\mathrm{vol}_{reservoir} + \mathrm{vol}_{matrix}(D-1))} \quad (2)$$

where C_v is the viable cell density measured by the biomass sensor, vol_{matrix} is the matrix volume, $\mathrm{vol}_{reservoir}$ is the reservoir volume, D is the perfusion rate. The IgG quantification was done by high-performance liquid chromatography (HPLC) Protein A method (Protein A column, Applied Biosystems, USA). Daily samples were purified and concentrated with NAb Protein A/G spin kit (Thermo Scientific, USA) and reducing sodium dodecyl sulfate-polyacylamide gel electrophoresis (SDS-PAGE) was performed. The cell specific consumption/production rates of nutrients/metabolites, the accumulated IgG production, the cell specific productivity and the volumetric productivity were calculated as previously described (Clincke et al., 2013a,b).

2.4.2. Microscopic observation of the cells and total cell enumeration

At the end of run, the CellTank was disassembled and the matrix disks were analyzed. Slices were orthogonally cut from each disk using a scalpel and microscopic analyses were carried out to study the cell distribution. The rest of the disks were cut into large pieces and placed in several shake flasks containing fresh medium, one disk in one flask. After vigorous shaking at 200 rpm for 30 min attempting to release all the cells from the matrix, the cell broths were analyzed by Bioprofile FLEX for a total cell number counting. The slices were observed under bright field microscope (inverted microscope Leica DMI6000b) at the cuts showing cells and cut fibers. The cells in the matrix were also fixed with 4% paraformaldehyde followed by DAPI fluorescent staining of the nuclei. The cell distribution was then observed by fluorescence microscopy up to a depth of 300 μm (inverted microscope Leica DMI6000b).

3. Results and discussion

3.1. Bioreactor design

A schematic representation of the CellTank is given in Fig. 1. The cells are entrapped in a non-woven spun-fiber polyester matrix in a cassette, which is immersed in a reservoir. The matrix is designed as a cylinder with two slightly angled envelopes containing 18 mm-thick stacked disks (totally 10 disks). The disks have 50 cm^2 inlet surface area and about 80 mL volume resulting in a total volume of 150 mL for the whole matrix. The culture medium is continuously circulating in the whole system: in the reservoir the liquid is pushed upwards into the matrix by a magnetically driven centrifugal pump under the cassette. The liquid enters into the cassette core center and flows orthogonally through each matrix disk as indicated in Fig. 1. After having passed the matrix, the liquid is collected at the median part of the matrix and then pushed into a rotameter, measuring the liquid recirculation mass flow. At the top of the rotameter, the liquid is pouring back into the reservoir, which gives a very effective exchange with the gas phase. During the perfusion mode, the recirculation of the liquid in the CellTank is very fast, 1.6 L/min, i.e., 10.7 VVM (volume per volume per minute) for a matrix volume of 150 mL. However the cells mostly remained trapped inside the porous matrix, captured in the tortuous flow path created by the series of interconnected void spaces of the micro filter structure. This fast recirculation flow ensures a homogeneous distribution of the fluid in the matrix. The centrifugal pump is manually operated at 250–600 rpm, resulting in a potential flow rate of 0–3 L/min. The required centrifugal pump effect to ensure the selected flow rate depends on the cell density: the higher the cell density, the higher the centrifugal pump rotation and power input. A power of 25 watts is required to overcome a 25 mbar pressure difference across the cell packed matrix in absence of cells. Sparging is operated in the reservoir. The sparged bubbles are never entering the matrix and are thus never in contact with the cells. The perfusion is carried out by adding fresh medium in the reservoir and removing conditioned medium from the rotameter, by two peristaltic pumps set at the same flow rate. In the present study, the pumps were run intermittently due to the small perfusion volumes, 150–1500 mL/day.

3.2. Cell density measurement by the biomass sensor

To our knowledge, the highest cell density measured by a Fogale bioimpedance biomass probe, that has been reported by off-line measurements is 20×10^6 cells/mL (Heinrich et al., 2011). However, in the present experiments, we reached densities well beyond this number. To confirm the reliability of the biomass measured by the biomass probe, we compared the cell density measured by this probe with suspensions of CHO DP-12 cells of different known cell densities. Cells exponentially grown in Erlenmeyer flasks were concentrated by centrifugation. The biomass sensor, 'on-line measurement', was placed in this concentrated cell culture and serial dilutions of the cell broth by medium were performed. The biomass readings were compared to the cell density measured using a Bioprofile FLEX instrument, 'off-line measurements' based on Trypan blue exclusion and image analysis. Each off-line measurement was an average of three values obtained by three different dilutions in fresh medium before measuring by Bioprofile FLEX. Fig. 2 was generated from duplicated experiments performed at different days. It shows that the reading from the biomass sensor agreed very well with the cell density measured by the Bioprofile FLEX up to 160×10^6 viable cells/mL, with 1 pF/cm corresponding to 1×10^6 viable cells/mL. Above this value the biomass sensor underestimated the cell densities and the biomass sensor reading saturated at a value around 203 pF/cm. Although this system was slightly different from the perfusion runs since fresh medium was used instead of conditioned medium, this comparison confirmed that 1 pF/cm was equivalent to 10^6 viable cells/mL up to 160×10^6 viable cells/mL density.

3.3. Investigation of CellTank performance limit and cell growth arrest

The purpose of run#1 was to test the CellTank and to study the cell density limit of the system. Run#2 aimed at studying the system behavior during cell growth arrest.

3.3.1. Cell density

Run#1 and run#2 were initiated by inoculating the reservoir with 150×10^6 viable cells, aiming at an initial cell density of 10^6 viable cells/mL in the 150 mL matrix. The recirculation flow was set to 1.0 L/min before the perfusion initiation, after which it was increased to 1.6 L/min and maintained at this value. Sampling from the reservoir 20 min after the inoculation showed that 75% of the

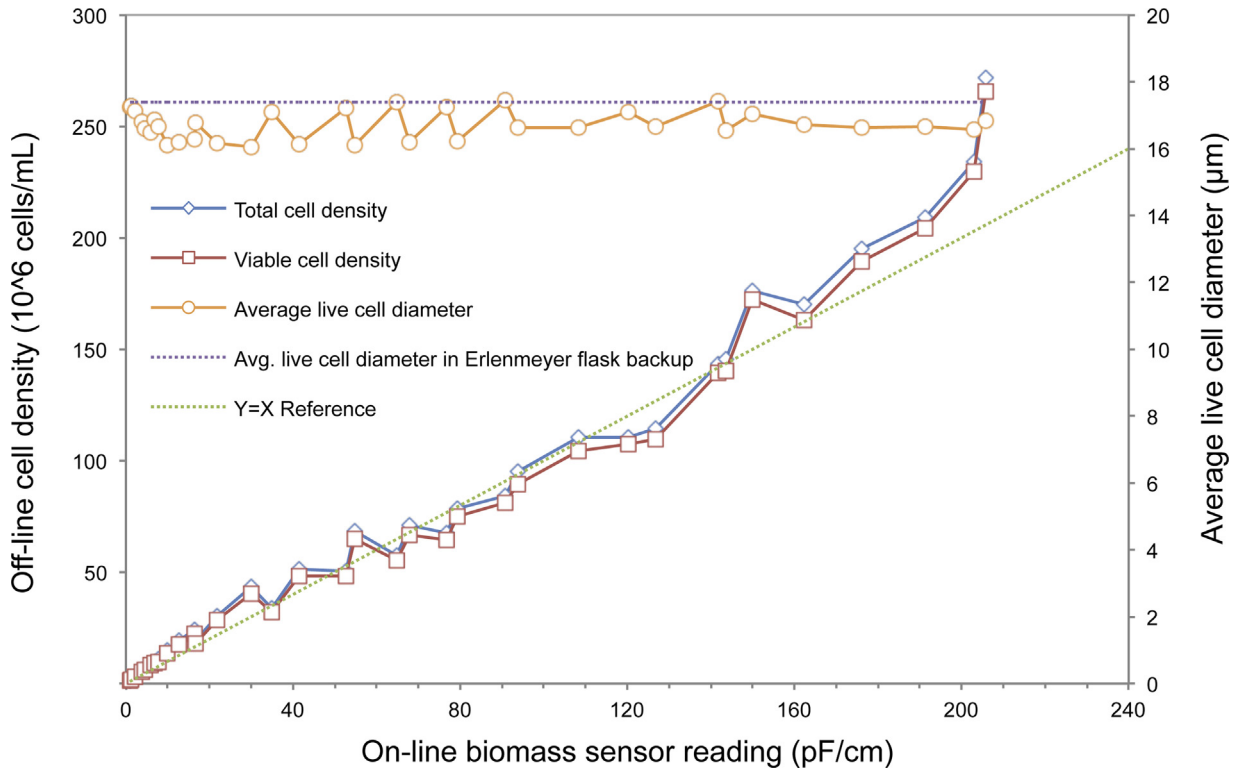

Fig. 2. Comparison of off-line measurements of the cell density by Bioprofile FLEX and on-line biomass sensor measurements by Fogale biomass probe in a concentrated cell suspension at different dilutions. The reference line Y = X or 10^6 viable cells/mL = 1 pF/cm is added for clarity. The curves include data from duplicates performed on different days.

cells were entrapped in the matrix and above 95% within 2 h following the inoculation.

Run#1 was a pioneer trial to study the system performance for a culture of cells in suspension and the capacity of the CellTank to support high cell densities. During the first two weeks of this run, the cell growth was slow due to troubleshooting and system adjustments, then from day 14, the cells grew exponentially. The cell density reached a maximal biomass reading of 200 pF/cm on day 26, see Fig. 3A. As presented above, the EVO reading was not linear with the cell density above 160×10^6 cells/mL but was underestimating the cell density. One can therefore affirm that the cell density was $\geq 200 \times 10^6$ viable cells/mL for the reading of 200 pF/cm. The density of the cells outside the matrix, i.e., in the reservoir was very low: $\leq 0.05 \times 10^6$ viable cells/mL before day 21 and up to 0.8×10^6 viable cells/mL after day 21, while the live cell density in the matrix was ≥82 pF/cm. The number of dead cells measured by LDH assay was low and increasing with time with a pattern roughly comparable to the viable cell density, resulting in a viability mostly ≥90 % during the whole run.

In run#2, the cells grew exponentially from day 1 (Fig. 3B). To study the potential of a process with cell density stabilized by cell growth arrest at high cell density in CellTank, a temperature shift study was carried out. The temperature was lowered from 37 °C to 32 °C when the biomass reading reached 97 pF/cm on day 10. This temperature notably reduced the growth. Further temperature reductions were then performed on day 11 to 31 °C, on day 14 to 30 °C and on day 16 to 29 °C, which eventually provoked a complete growth arrest. The hypothermia resulted in a viable cell density stabilized around 130 pF/cm maintained for 9 days, from day 14 to day 22. The cell viability was ≥90% during the whole run. The number of cells leaking from the matrix, represented in Fig. 3B, was very low compared to the number of cells entrapped in the matrix: It increased slightly from 0.1×10^6 cells/mL to 0.3×10^6 cells/mL after the temperature reduction on day 10 and increased up to 1.2×10^6 cells/mL after day 20.

3.3.2. *Perfusion rate and recirculation rate*

The perfusion was initiated at a rate of 1 RV/day and then increased linearly with the cell density. Further increases of the perfusion rate were also performed to reduce the by-product levels as described in Section 2. In run#1, at 200 pF/cm the perfusion rate was 10 RV/day on day 25. In this run, the perfusion rate was increased at a value higher than the CSPR (Eq. (1)) on day 5 and day 21 when the ammonia level reached 4.8 mM and 6 mM, respectively (Fig. 4B).

In run#2, the perfusion rate was adjusted according to Eq. (1) except two times, when the ammonia level reached 5 mM on day 5 and when the lactate and ammonia levels reached 50 and 8 mM respectively on day 8, see Fig. 4C and D. Noticeably despite a reduced metabolism, consecutive to the growth arrest, the lactate concentration increased hence the perfusion rate was increased accordingly up to 10 RV/day. Reducing the perfusion rate to 8 RV/day on day 21 resulted in a new increase of the lactate level.

The recirculation rate was measured by reading of the rotameter and manually controlled by adjusting the centrifugal pump stirring speed. Table 1 shows the relationship between the cell density in the matrix, the recirculation flow, the pressure inside the matrix, and the centrifugal pump stirring speed. The stirring speed was constant and the pressure at the outlet of the centrifugal pump was stable, around 0.030 bar, during the exponential cell growth until 100×10^6 cells/mL, i.e., until day 10. After that day, the pressure obtained from the centrifugal pump to maintain the recirculation rate at its 1.6 L/min set point, was incrementally increased every day: an increase of approximately 15 rpm per day of the stirrer speed was needed to ensure this required pressure. A very high

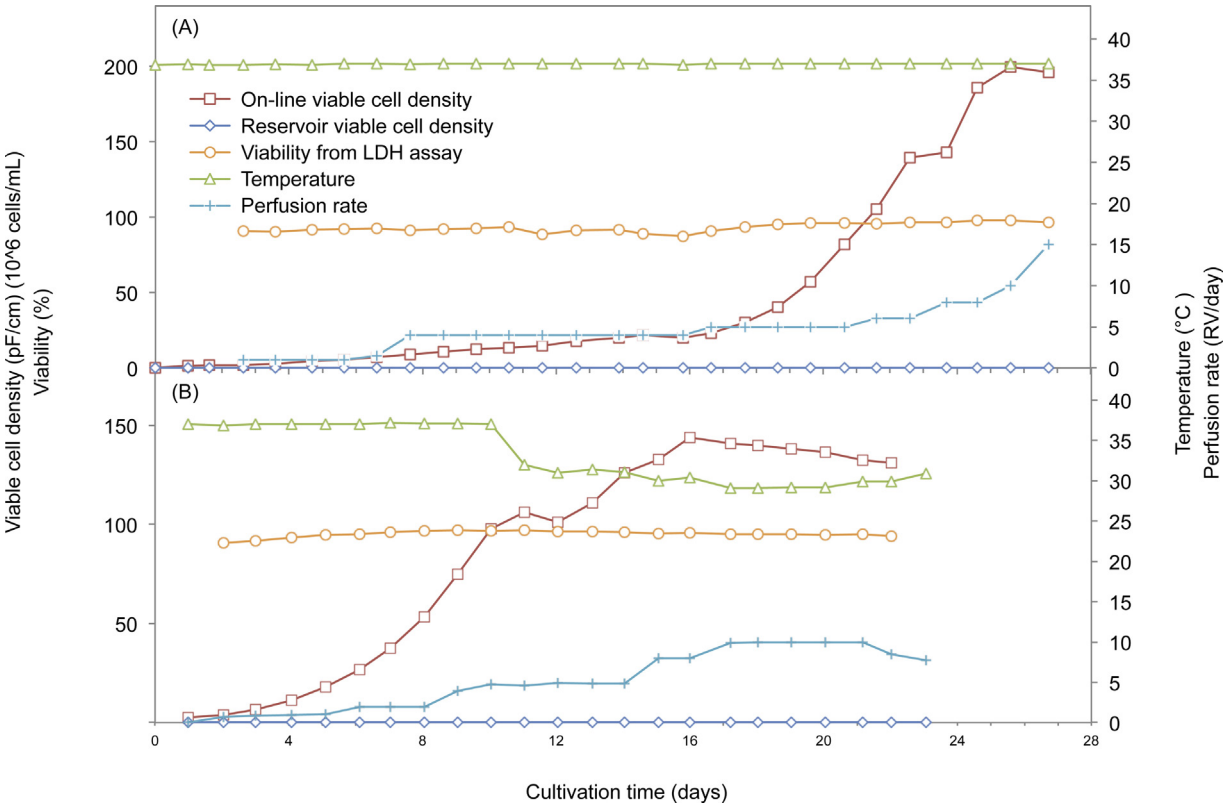

Fig. 3. Cell growth profiles for run#1 and run#2. (A) Run#1; (B) run#2.

Table 1
Cell density, recirculation flow, pressure, and stirring speed for run#2 with temperature lowered gradually.

Time (days)	Cell density (pF/cm)	Mass flow (L/min)	Pressure (mm)	Stirring speed (rpm)	Theoretical pressure (bar)
1	2.61	1.6	300	300	0.029
2	3.82	1.6	305	300	0.030
3	6.52	1.6	310	300	0.030
4	11.35	1.5	295	300	0.029
5	18.08	1.6	315	300	0.031
6	26.75	1.6	310	300	0.030
7	37.38	1.5	305	300	0.030
8	53.23	1.6	305	300	0.030
9	74.81	1.5	330	300	0.032
10	97.68	1.6	330	300	0.032
11	106.03	1.6	350	325	0.034
12	101.1	1.5	370	340	0.036
13	110.78	1.6	380	355	0.037
14	125.94	1.5	385	370	0.038
15	132.77	1.5	350	385	0.034
16	143.77	1.55	420	400	0.041
17	140.88	1.6	440	425	0.043
18	139.98	1.6	450	440	0.044
19	138.08	1.5	460	440	0.045
20	136.65	1.5	450	450	0.044
21	132.33	1.6	470	460	0.046
22	131.24	1.6	470	460	0.046
23	129.36	1.6	490	460	0.048

torque was finally required from the magnetic stirrer towards the end of the run to push the recirculation medium through the matrix.

It is probable that the required pressure increased due to the physical hindrance created by the cells and the cell debris inside the matrix.

3.3.3. *Information of the biomass sensor*

The principle of dielectric spectroscopy and the β-dispersion model of the permittivity measurement have been abundantly described elsewhere (Ansorge et al., 2007; Carvell and Dowd, 2006; Ducommun et al., 2002a; Harris et al., 1987; Kaufmann et al., 1999; Noll and Biselli, 1998; Sarra et al., 1996; Zeiser et al., 1999) and used to determine the cell density in suspension or in adherence on microcarriers in bioreactor. One of the key parameters, the characteristic (or critical) frequency f_c, is calculated from the permittivity scanning data and is always regarded as a reciprocal indicator of cell size. Cole–cole *alpha* is an empirical parameter considered as an indicator of the size homogeneity (Markx et al., 1991). The readings measured by the biomass sensor for run#1 are given in Fig. 5. From day 16, f_c declined, suggesting that the cells became larger.

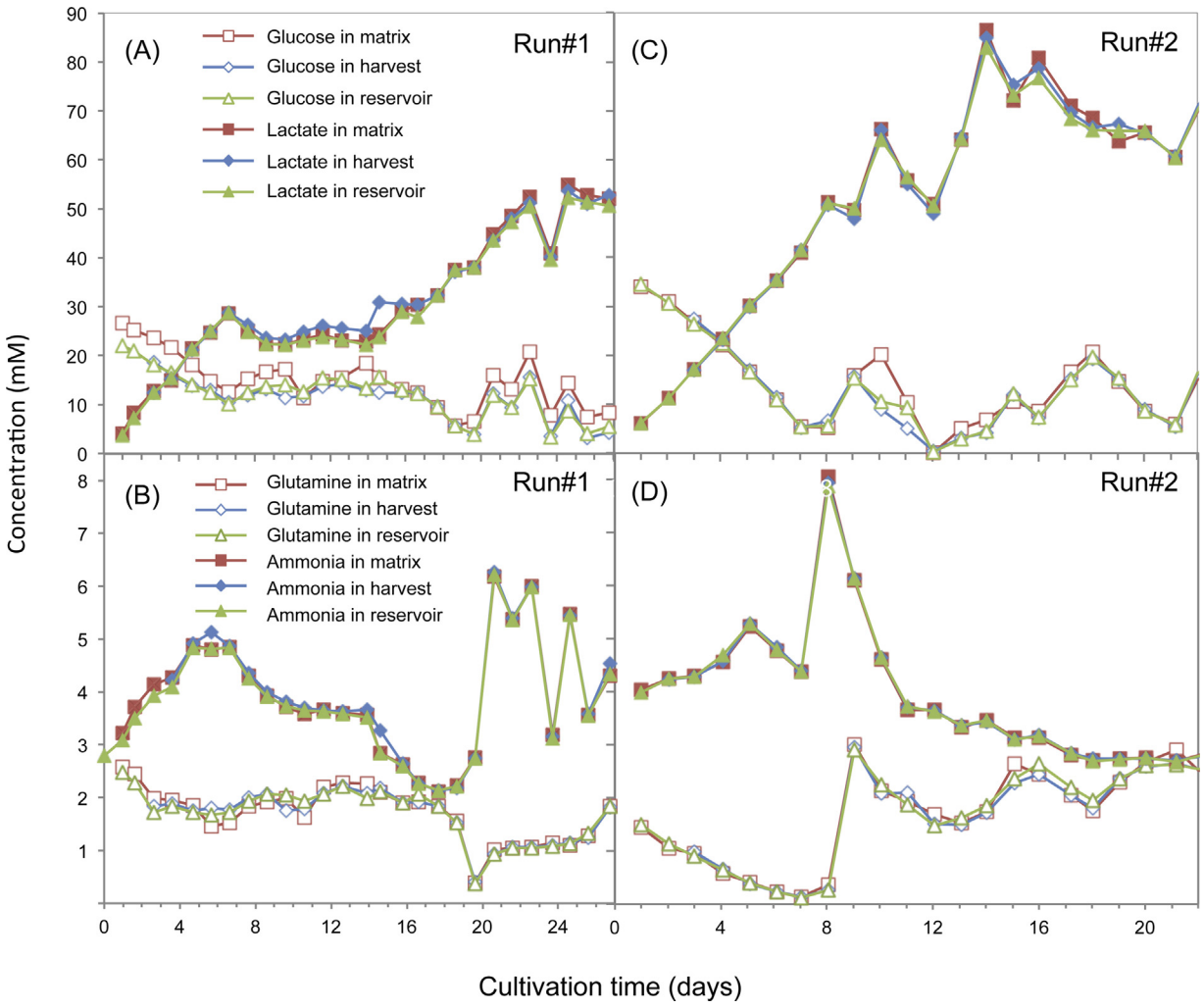

Fig. 4. Metabolites/nutrients profiles for run#1 and run#2 from three different sampling locations: matrix, harvest line and bottom of the reservoir. (A) Glucose and lactate concentrations in run#1; (B) glutamine and ammonia concentrations in run#1; (C) glucose and lactate concentrations in run#2; (D) glutamine and ammonia concentrations in run#2.

During the cultivation, cole–cole *alpha* was increasing, indicating an increasing inhomogeneity of the cell sizes. At the high cell density of 200 pF/cm, an upper limit of 1000 pF/cm of the permittivity variation DeltaEps was reached, leading to the saturation of the biomass reading. From day 19, the conductivity began to decrease, dropping to almost half its starting value at the end. This might be associated to a modification of the ion cellular uptake from the medium. Finally, a very high correlation between the biomass (calculated from 2 frequencies) and DeltaEps (all frequencies) was observed.

3.3.4. IgG production

The IgG concentrations in the bioreactor as well as the cell specific productivities (q_{IgG}) are represented in Fig. 6. The IgG concentrations in the matrix and in the harvest line were comparable hence a yield close to 100% was obtained indicating no retention of the IgG in the bioreactor. The q_{IgG} was in average 1.7 pg/cell/day in run#1 as well as in run#2 until day 14. This value was comparable or slightly higher than the q_{IgG} of 1.5 pg/cell/day measured in Erlenmeyer flask batch cultures. When the temperature was decreased to 30 °C in run#2, q_{IgG} increased to an average of 2.5 pg/cell/day, i.e., 47% higher than at 37 °C. When the temperature was further lowered to 29 °C from at day 16, q_{IgG} decreased to ≈2 pg/cell/day. Thus the optimal temperature maximizing the cell specific productivity was 30 °C for this cell line.

To study if fragmented variants occurred when the cell density was increased, reducing SDS-PAGE was performed for both runs, see Fig. 7A and B. These analyses were repeated showing exactly the same results (data not shown). As can be seen in Fig. 7, both the heavy chain and light chain bands showed high similarities from 27 pF/cm to 200 pF/cm biomass readings at 37 °C temperature. A faint band ("2nd band" in Fig. 10B) with a slightly lower molecular weight than the main light chain band ("1st band"), increased in intensity with decreasing temperatures. The 2nd band became stronger at 30 °C temperature and even darker than the 1st light chain band at 29 °C. These results indicate that no fragment variant occurred at 37 °C culture temperature up to 200 pF/cm biomass reading. A variant of the light chain was observed when hypothermia was applied, with an intensity increasing with decreasing temperature.

3.3.5. Cell metabolism

The concentrations of glucose, lactate, glutamine and ammonia measured during run#1 and run#2 are shown in Fig. 4. These concentrations were comparable in the matrix, the harvest line and in the bottom of the reservoir, illustrating that the fluid composition was homogeneous in the whole system. The lactate increased with time in run#1 and finally reached 52 mM. In run#2, it increased to 86 mM on day 14 after which it decreased. The ammonia concentration became suddenly very high, 6.2 mM on day 21 in run#1

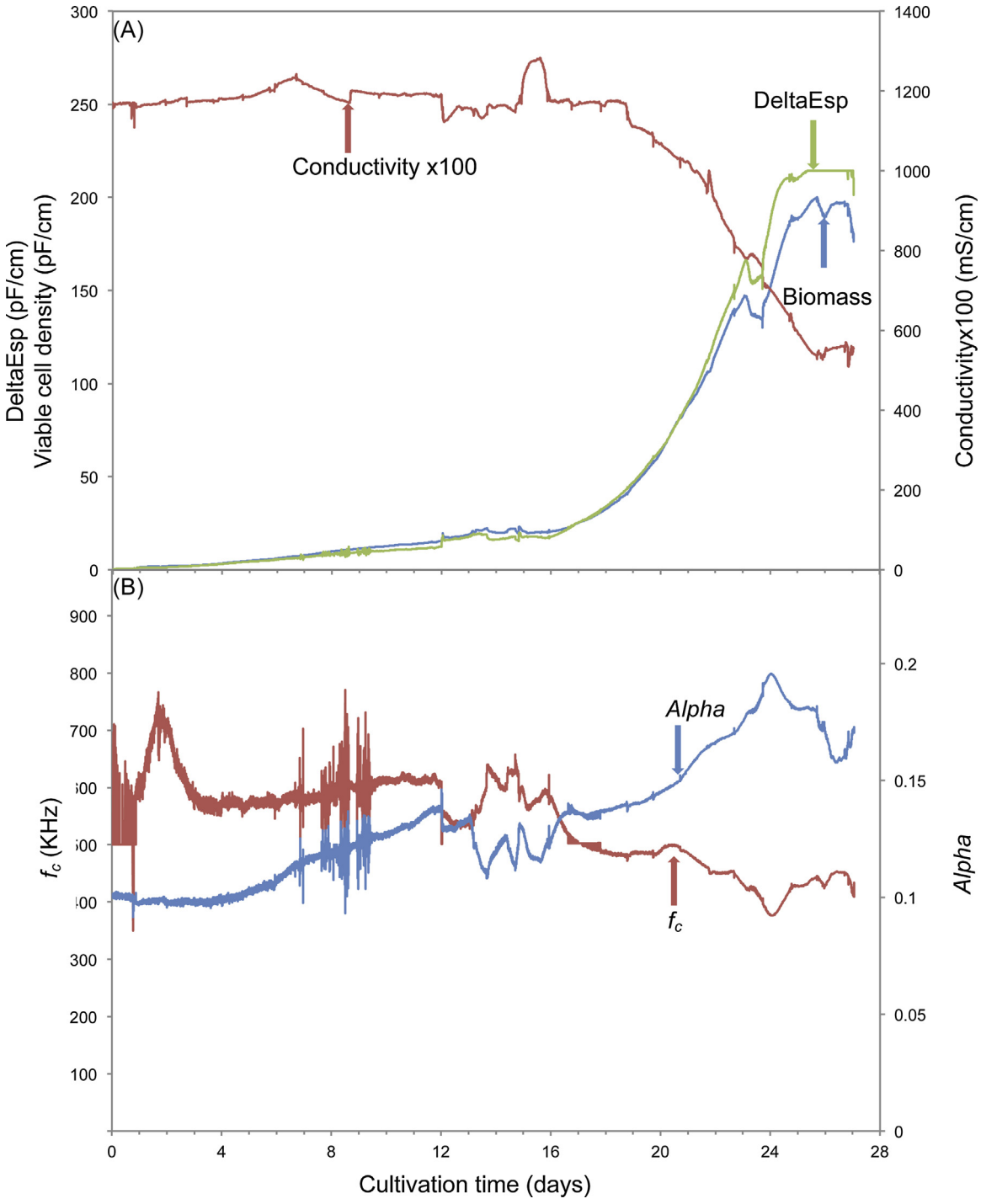

Fig. 5. On-line biomass sensor monitoring. (A) Biomass, culture conductivity (multiplied by 100 to fit the scale) and DeltaEsp. The biomass was calculated by the iBiomass 200 system from measured permittivity data, which subtracted the permittivity of the experiment medium without any cells. The DeltaEsp was the permittivity variation measured to calculate other parameters; (B) f_c and *alpha*.

and 8 mM on day 8 in run#2. In both cases, glutamine had been almost depleted and additional supplementations were performed followed by sudden ammonia increase the next day. Likewise an abrupt ammonia increase was observed on day 5 in run#2 after glutamine had been fed on day 4, although not depleted.

The high levels of lactate and ammonia were probably due to the presence of glucose and glutamine at relatively high concentrations, as showed by their residual concentrations of up to 20 mM and 3 mM, respectively.

3.4. Production run at high density of growth-arrested cells

A production run, run#3, was conducted based on the learning's from run#1 and run#2.

From run#2, it was known that the CellTank supported high cell density culture under cell growth arrest by temperature. Run#1 showed that the CellTank supported densities up to 200×10^6 cells/mL hence selecting a density between 100 and 140×10^6 cells/mL allowed a large failure margin. It was decided to select a production process including cell growth arrest since this

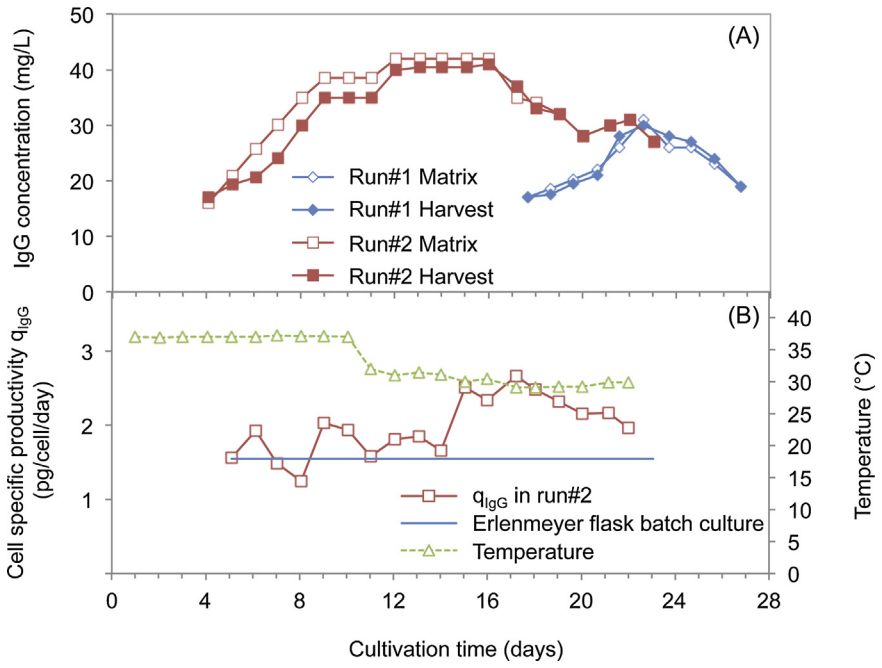

Fig. 6. IgG production profiles for run#1 and run#2. (A) IgG daily concentrations from both matrix and harvest; (B) cell specific productivities q_{IgG} in run#2 compared with the average cell specific productivity obtained in batch cultures from Erlenmeyer flasks.

type of process has the potential to generate a stable and long-term IgG production while a cell bleeding procedure from the matrix was not available.

It was observed in run#2 that the optimal temperature maximizing the cell specific productivity was 30 °C for this cell line. However, the results from this run showed some cell viability drop at temperature ≤30 °C. Therefore the hypothermia temperature finally selected for run#3 was 31 °C. Run#3 included a growth phase, phase 1, followed by a two-weeks production phase at 31 °C hypothermia, phase 2, initiated when the cell density reached 100 pF/cm biomass reading. Towards the end of the run, the temperature was restored to 37 °C to verify that the cells growth could be re-initiated, phase 3. Finally, in run#3, the feed strategy of the substrates was modified compared to the previous runs to reduce the production of the by-products: the feeds of glucose and glutamine were minimized.

3.4.1. Cell density

To reduce the time to achieve the target density of 100 pF/cm, the culture was inoculated at 2×10^6 cells/mL. At day 13, the cell density reached 97 pF/cm with a viability of 89% and the temperature was decreased to 31 °C. At days 11 and 12, the cell growth decreased somewhat as well as the viability. After the temperature shift, the cell growth was significantly reduced as can be seen in Fig. 8 and stabilized around 100–120 pF/cm during 14 days. The viability decreased with time down to 73.4% at day 27. The cell density in the reservoir slightly increased after the temperature shift until a concentration of 0.55×10^6 cells/mL at day 27.

At day 28, the temperature was restored to 37 °C. After 3 days of lag phase, the cell growth resumed however at a slower pace than before day 13.

After completion of the run, the CellTank was disassembled and all the disks of the matrix were individually removed. The cell distribution in the disks and the total number of cells in the matrix were analyzed as described in Section 2. A total number of about 130×10^6 cells/mL were counted in the matrix. This number was similar to the final biomass reading from the on-line biomass probe, 152×10^6 cells/mL. It was not possible to completely dislodge all the cells from the matrix, however recovering 130×10^6 cells/mL supported the final reading from the biomass probe.

The cell distribution in the disk was analyzed by observing slices cut in the disk and by fixing the cells in the matrix. It was observed that the cells were loose inside the matrix, i.e., not adhering, and were immediately released after the matrix had been cut. All the disks exhibited a comparable and homogeneous distribution of the cells through the disk and through the matrix although the bottom disk exhibited somewhat more cell aggregates compared to the other disks. This is illustrated in Fig. 9A–D showing four different depths in the matrix: top (disk 1), median level (disks 5 and 6) and bottom (disk 10). Fig. 9E illustrates how the cells were located in the interstices of the matrix fibers, showing DAPI staining of the cell nuclei. Note that Fig. 9E picture was taken at a single plane so some parts appear blurry. A stack of 56 pictures with 85.90 μm depth along the *Z*-axis helps to visualize the distribution of cells inside the matrix in a deeper view (Zhang et al., 2015).

3.4.2. IgG production

At the end of the production phase 2 as shown in Fig. 10A, at day 27, 1.42 g IgG had been harvested in the 150 mL CellTank prototype with a total expense of 13 L medium. It was confirmed that the concentration in the harvest line was similar to the one measured in the matrix, leading to a 100% yield (data not showed).

3.4.3. Cell metabolism

Low glucose and glutamine feeds were adopted to minimize the production of lactate and ammonia. The residual concentrations of these substrates were 0 mM glucose from day 7 and between 0 and 0.6 mM glutamine most of the time as in Fig. 10B and C. Notice that although their residual concentrations were very low, these substrates were provided to the culture from the medium. The applied perfusion rates obeyed consistently Eq (1). The residual lactate concentration was almost constant at a value lower than 40 mM during the production phase at hypothermia, while the ammonia concentration increased up to 5 mM.

It is probable that the metabolism shifted towards an increased catabolism of the amino acids into the TCA cycle to compensate

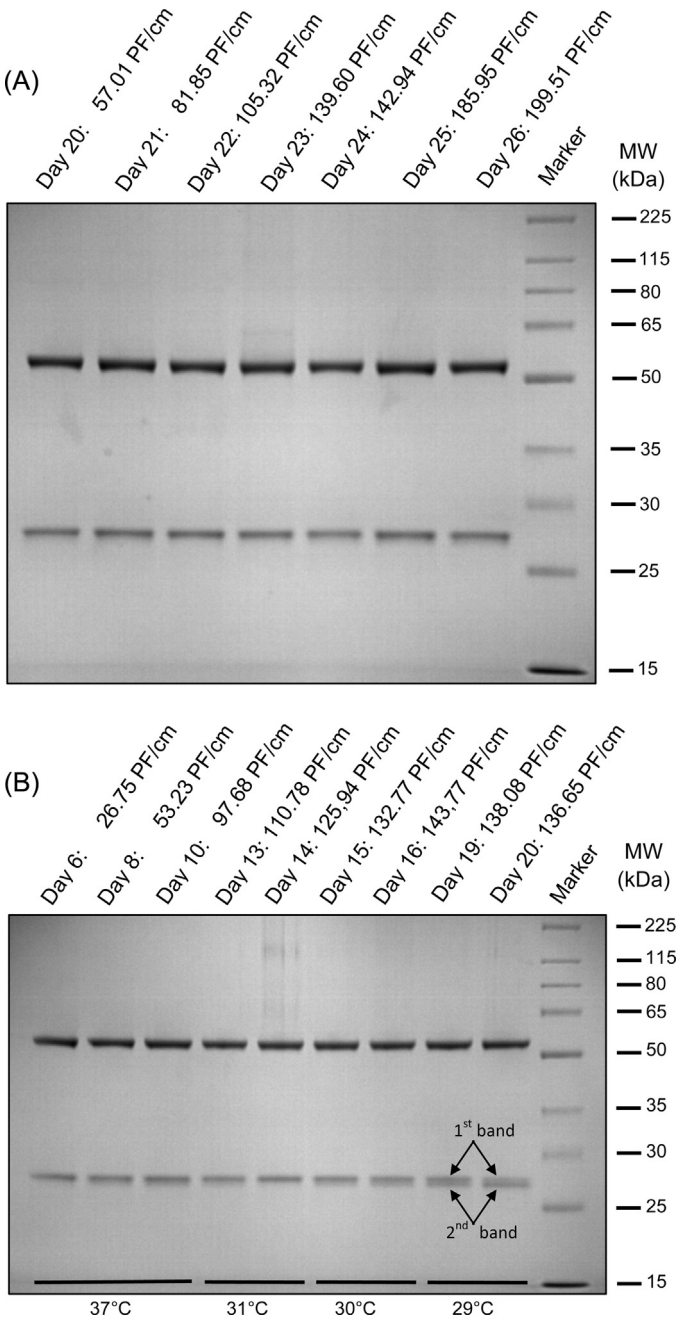

Fig. 7. Reducing SDS-PAGE gel electrophoresis showing the light and the heavy chains of the IgG. (A) Daily samples from day 20 to day 26 with cell density label from run#1; (B) daily samples with cell density and temperature label from run#2.

for the low glucose availability, generating a higher production of ammonia.

4. Discussion

The CellTank was a bioreactor easy to operate, with the advantages of integrating the cell separation device, reducing the complexity compared to systems with external cell separation device or external pumps for the recirculation. The centrifugal pump offered an attractive alternative to the peristaltic pump for the cells not entrapped in the matrix, avoiding the shear effect of the pump head and the wall shear stress from recirculation in the tube system. A drawback of the cell entrapment was the absence of cell sampling, requiring a supplementary method to measure the biomass. In this study, this was solved using a bioimpedance measurement in the matrix.

4.1. Cell density

A cell density up to 200×10^6 cells/mL was obtained in run#1 and cell densities between 100 and 140×10^6 cells/mL were maintained during 11 and 14 days under cell growth arrest in runs #2 and #3. The cell growth was slightly slower in run#3 compared to run#2 at cell density above 75×10^6 cells/mL however in both cases 100×10^6 cells/mL were successfully achieved. The cell viability was mostly higher than 90 % during runs #1 and #2. During run#3, it decreased after day 12 and was 73.4 % at the end of the two-weeks production phase under hypothermia. The cause of the lower viability is not known. It can be speculated that the shear stress is high in the system, in particular when the interstices between the fibers are reduced from the cell presence. The recirculation rate was set to 1.6 L/min however, at this stage, it has not been optimized but could potentially be reduced in future work.

Most of the high cell densities above 100×10^6 cells/mL reported in perfusion-integrated systems with immobilize or entrap cells, have been achieved using hybridoma cells (Oh and Chang, 1992; Wang et al., 1992; Zhu and Yang, 2004). The average cell diameter for hybridoma cells is 15 μm while the average live cell diameters for the cell line used in the present study was 17 μm, as shown in Table 2. In an earlier study we have presented the theoretical fraction of the volume occupied by the cells in a cell suspension as a function of the cell diameter. From this study, with a cell diameter of 15 μm, hybridoma cells at density of 187×10^6 and 101×10^6 cells/mL, occupy a fraction of 0.330 and 0.178, respectively, while at 200×10^6, this fraction is 0.514 for CHO cells with 17 μm diameter (Clincke et al., 2013b). The maximal biovolume reported in the present study was thus much larger than previously described. Additionally, the present results can also be benchmarked against fibrous-bed bioreactor where 101×10^6 hybridoma cells/mL has been reached (Zhu and Yang, 2004). Although these perfusion systems present the common feature of immobilizing the cells in larger matrices like in the CellTank, the very efficient recirculation flow of the CellTank enabled obtaining by far higher cell densities and much more homogeneous environmental culture conditions as showed by similar profiles of the metabolites measured at different locations of the CellTank.

Finally, the CellTank system can also be compared to stirred tank bioreactor using other types of perfusion devices such as ATF or TFF. We have not performed a direct comparison of these systems with this cell line. As a benchmarking, it can be mentioned that in all these systems, i.e., CellTank, ATF, TFF, we have obtained cell densities by far above 100×10^6 cells/mL, i.e., up to $180–214 \times 10^6$ cells/mL (Chotteau et al., 2013; Clincke et al., 2013a,b). Although, the cell growth rate was somewhat slower in run#3 above a density of 75×10^6 cells/mL, the CellTank could support comparable cell growth as the ATF or TFF.

4.2. Perfusion rate, recirculation rate and feeding approach

The perfusion rate (calculated based on the matrix volume) was tuned linearly with the cell density using a CSPR approach, except when the by-product concentrations became too high in runs #1 and #2. In run#3, a CSPR around 0.05 nL/cell/day was consistently applied. In this last run, a strategy of low substrate feeding was also adopted: glucose and glutamine were scarcely added resulting in low residual concentrations of these substrates. This led to moderate production of lactate and ammonia. CSPR strategy to tune the perfusion rate has been successfully applied previously for very high cell densities (Clincke et al., 2013b). Here it was shown that it

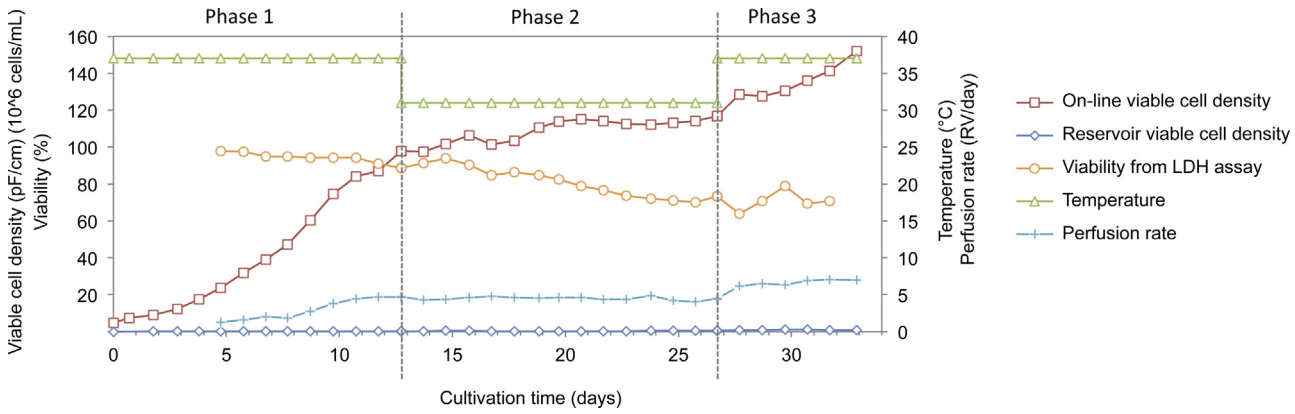

Fig. 8. Cell growth profiles in run#3. Phase 1: cell growth phase; phase 2: production phase at temperature 31 °C; phase 3: new growth phase at temperature 37 °C.

could be applied for the CellTank as well, given that the substrate feeds were limited.

The metabolite concentrations were similar in different locations of the CellTank, demonstrating that no gradient occurred in the system. This presents a major advantage compared to other systems where the cells are entrapped or immobilized, since the gradients of substrates, gases and by-products can create local conditions unfavorable for cells or the productivity, and can cause non-homogeneous product quality.

A recirculation rate of 1.6 L/min was applied however this value was not optimized in this first proof-of-concept study. It is possible that the shear stress associated to this recirculation rate was too high and could possibly cause the lower viability observed in run#3. It will be interesting in future work to decrease this rate.

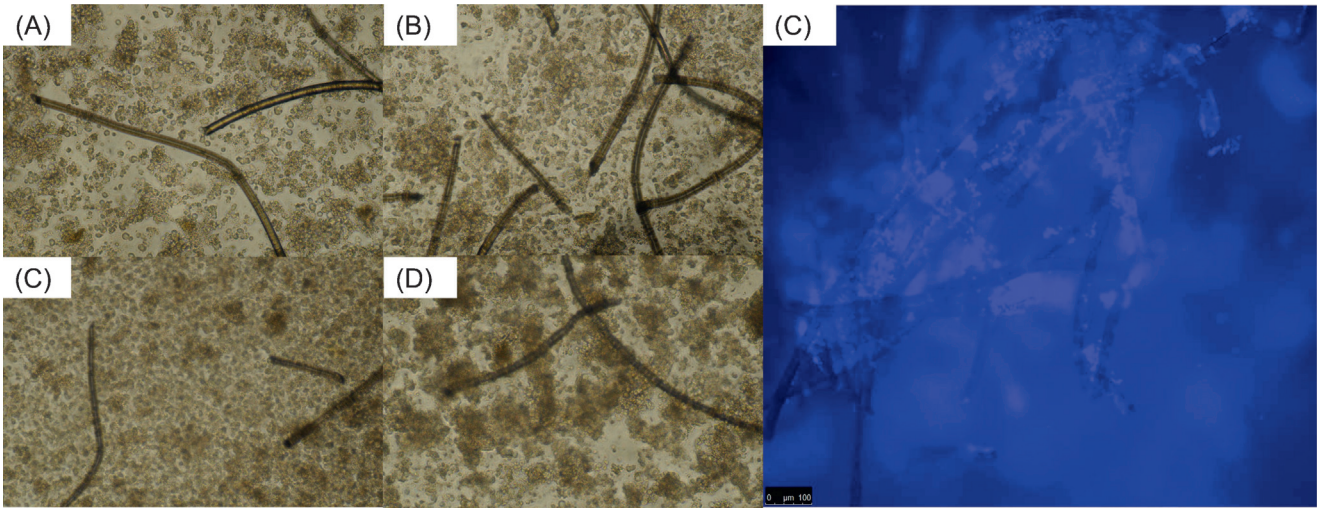

Fig. 9. Cells distribution inside the matrix visualized in slices cut in top disk (A); upper middle disk (B); lower middle disk (C); bottom disk (D). Only fiber pieces are visible in the cuts. (E) DAPI fluorescence staining showing the distribution of the cells in the interstices between the fibers.

Table 2
Average live cell diameters measured by Bioprofile Flex with window 13 μm-20 μm for min.-max. cell size based on off-line image analysis for matrix samples.

Run#1	Average Cell Diameter (μm)	Run#2	Average Cell Diameter (μm)
Day 14	17.04	Day 7	16.60
Day 15	17.63	Day 8	17.06
Day 16	17.38	Day 9	16.26
Day 17	18.27	Day 10	16.84
Day 18	17.78	Day 11	16.95
Day 19	17.18	Day 12	16.67
Day 20	16.16	Day 13	16.75
Day 21	16.97	Day 14	17.00
Day 22	16.65	Day 15	16.71
Day 23	16.75	Day 16	16.17
Day 24	16.96	Day 17	16.82
Day 25	16.78	Day 18	17.26
Day 26	17.1	Day 19	17.44
Day 27	17.09	Day 20	17.48
		Day 21	17.48
		Day 22	17.31

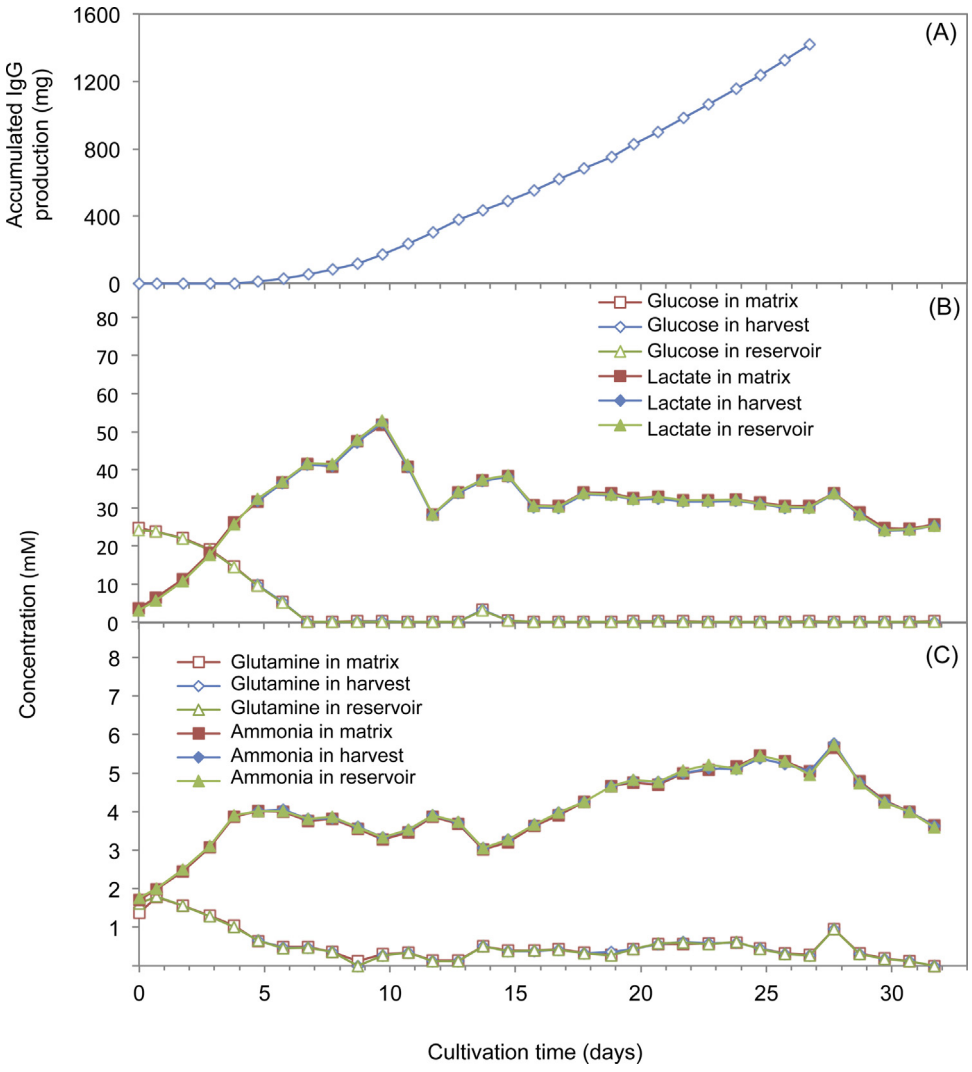

Fig. 10. Accumulated IgG production and metabolites/nutrients profiles from three sampling locations during run#3. (A) Accumulated IgG until the end of the production phase; (B) glucose and lactate concentrations; (C) glutamine and ammonia concentrations.

4.3. IgG production

An IgG production of 1.42 g was achieved during a production run in a matrix bioreactor of 150 mL volume using the low producer CHO cell line DP12. Using the same cell line, we measured in a productivity test that a batch process would have generated 54 mg/L after a 6-days batch production run reaching 6.15×10^6 cells/mL in shake flask. In other words, for a production campaign of 30 days, 40.5 mg IgG could be produced in a volume of 150 mL, compared to a production of 1.42 g achieved using the CellTank, i.e., 35 fold more product during the same time period.

No IgG retention was observed in the system. Retention of the product of interest is an important issue for filter-based cell retention devices where it is often observed and aggravated at higher cell densities (Clincke et al., 2013a; de la Broise et al., 1992). The absence of retention in the CellTank system is a favorable feature, which could be due to the fast recirculation flow or to the matrix material, i.e., polyester, or to a combination of these factors.

A hypothermia strategy was applied to arrest the cell growth and enhance the production. The CellTank, in its present version, does not allow easy detaching and harvesting the cells during the operation. To decrease the temperature is thus an efficient way to control the cell density as has been showed by others (Ducommun et al., 2002b). The effect of temperature shift depends on the cell line. In the present study, we successfully showed that it was possible to lower the temperature to arrest the cell growth at cell densities $\geq 100 \times 10^6$ cells/mL and to increase the cell specific productivity. Reducing progressively the temperature was a simple method to identify the optimal production temperature.

We observed that no fragment variant occurred in the culture at 37 °C up to the very high density of 200×10^6 cells/mL. Hypothermia was associated with the occurrence of a variant of the light chain with an intensity increasing with decreasing temperature. Variations in the IgG light chain glycosylation have been reported (Holland et al., 2006; Jefferis, 2005, 2009; Mimura et al., 2007; Rustandi et al., 2008; Tachibana et al., 1993) and hypothermia is known to be a potential cause of these variations (Ahn et al., 2008; Bollati-Fogolin et al., 2005; Tharmalingam et al., 2008; Trummer et al., 2006; Yoon et al., 2003). It is highly probable that the light chain variations observed here were due to a different glycosylation.

5. Conclusions and perspective

A new disposable perfusion bioreactor, CellTank, integrating the cell separation device was investigated. In this system, the cells were entrapped in a non-woven polyester matrix, perfused by the culture medium. In this current study, three runs were

performed at cell densities above 100 pF/cm, where 1 pF/cm was equivalent to 1×10^6 viable cells/mL up to a cell density of 160×10^6 cells/mL. In the first run aimed at studying the cell density capacity of the bioreactor, a maximal cell density of 200 pF/cm was reached. In the second run, hypothermia at temperature $\leq 32\,^{\circ}C$ was applied to the culture to arrest the cell growth and to increase cell productivity. The density stabilized between 100×10^6 and 130×10^6 cells/mL during 13 days. Hypothermia at 31 °C was selected for a production run, run#3, applied after the cell density reached 100×10^6 cells/mL. Despite the use of a cell line adapted to cell suspension and a very fast recirculation flow of 1.6 L/min between the matrix and the reservoir, i.e., 10.7 VVM (volume per volume per minute), the cells mostly remained entrapped inside the matrix. It was observed that when the cell growth was partially arrested by hypothermia, a higher proportion of the cells were dislodged from the matrix. The bioreactor had been designed to achieve a homogeneous distribution of the medium component in the whole system and it was indeed demonstrated that no gradients occurred in this system even at very high cell densities. No IgG retention in the bioreactor was observed up to a cell density of 200 pF/cm.

Inherently to the concept of the CellTank, based on cell entrapment, there was no way to operate cell bleeding to maintain the cell density at a stable level. During the operation, it was observed that increasing the recirculation rate could provoke the cell detachment from the matrix, in particular when abrupt variations of this rate were applied (data showed). This feature could be systematically exploited in future work to enable the cell detachment to harvest or bleed the cells.

The scale-up of the system was not studied in the present proof-of-concept study but theoretical considerations can be made here. The system can be enlarged in height and in diameter. The 150 mL CellTank contains two envelopes including five disks each and oriented with angles optimized to obtain a homogeneous and efficient flow distribution. The system can be enlarged by adding supplementary double envelops (each containing two times five disks) in height, i.e., increasing the height of the cassette to include a larger number of disks, while enlarging the centrifugal pump capacity and power input. This scale-up is only an extension of the actual design and can generate a matrix volume of 15×150 mL, i.e., 2250 mL. The enlargement of the system in diameter will require a new optimization of the envelope design.

The CellTank is a compact system for the production of biologics, supporting very high cell densities, with the capacity to be enlarged to several liters. The bioreactor settings do not require a cell specific optimization. In a one-month campaign, the 150 mL CellTank has the capacity to generate several grams of product of interest, depending on the cell specific productivity. Hence this system can be used to produce material for diagnostics, as research tool or for early stage manufacturing. The field of application of the up-scaled CellTank will be the production of several tens to hundreds of grams of product of interest.

Conflict of interest

There is no conflict of interest in this paper.

Acknowledgements

This work was financed by the Swedish Governmental Agency for Innovation Systems (VINNOVA). We thank Belach Bioteknik for lending a Biophantom process control system (Sweden). We are also grateful to Fogale Nanotech (France) and their representative Bent Svanholm, Svanholm.com (Denmark) for lending the iBiomass 200 system.

References

Ahn, W.S., Jeon, J.J., Jeong, Y.R., Lee, S.J., Yoon, S.K., 2008. Effect of culture temperature on erythropoietin production and glycosylation in a perfusion culture of recombinant CHO cells. Biotechnol. Bioeng. 101, 1234–1244.

Ansorge, S., Esteban, G., Schmid, G., 2007. On-line monitoring of infected Sf-9 insect cell cultures by scanning permittivity measurements and comparison with off-line biovolume measurements. Cytotechnology 55, 115–124.

Bohak, Z., Kadouri, A., Sussman, M.V., Feldman, A.F., 1987. Novel anchorage matrices for suspension-culture of mammalian-cells. Biopolymers 26, S205–S213.

Bollati-Fogolin, M., Forno, G., Nimtz, M., Conradt, H.S., Etcheverrigaray, M., Kratje, R., 2005. Temperature reduction in cultures of hGM-CSF-expressing CHO cells: effect on productivity and product quality. Biotechnol. Progress 21, 17–21.

Carvell, J.P., Dowd, J.E., 2006. On-line measurements and control of viable cell density in cell culture manufacturing processes using radio-frequency impedance. Cytotechnology 50, 35–48.

Castilho, L.R., Medronho, R.A., 2002. Cell retention devices for suspended-cell perfusion cultures. Adv. Biochem. Eng. Biotechnol. 74, 129–169.

Chen, C., Huang, Y.L., Yang, S.T., 2002. A fibrous-bed bioreactor for continuous production of developmental endothelial locus-1 by osteosarcoma cells. J. Biotechnol. 97, 23–39.

Chen, Z.L., Wu, B.C., Liu, H., Liu, X.M., Huang, P.T., 2004. Temperature shift as a process optimization step for the production of pro-urokinase by a recombinant Chinese hamster ovary cell line in high-density perfusion culture. J. Biosci. Bioeng. 97, 239–243.

Choi, S.K., Chang, H.N., Lee, G.M., Kim, I.H., Oh, D.J., 1995. High cell density perfusion cultures of anchorage-dependent vero cells in a depth filter perfusion system. Cytotechnology 17, 173–183.

Chotteau, V., 2015. In: Al-Rubeai, M. (Ed.), Perfusion Processes in Animal Cell Culture. Springer Intl.

Chotteau, V., Clincke, M., Zhang, Y., Thoring, L., 2013. Achievement of extreme cell densities in different perfusion systems and impact of the cell density. In: ECI Conference I - Integrated Continuous Biomanufacturing, Castelldefels.

Chu, L., Robinson, D.K., 2001. Industrial choices for protein production by large-scale cell culture. Curr. Opin. Biotechnol. 12, 180–187.

Clementschitsch, F., Bayer, K., 2006. Improvement of bioprocess monitoring: development of novel concepts. Microb. Cell Fact. 5.

Clincke, M.F., Molleryd, C., Samani, P.K., Lindskog, E., Faldt, E., Walsh, K., Chotteau, V., 2013a. Very high density of Chinese hamster ovary cells in perfusion by alternating tangential flow or tangential flow filtration in WAVE Bioreactor-part II: Applications for antibody production and cryopreservation. Biotechnol. Progress 29, 768–777.

Clincke, M.F., Molleryd, C., Zhang, Y., Lindskog, E., Walsh, K., Chotteau, V., 2013b. Very high density of CHO cells in perfusion by ATF or TFF in WAVE bioreactor. Part I. Effect of the cell density on the process. Biotechnol. Progress 29, 754–767.

de la Broise, D., Noiseux, M., Massie, B., Lemieux, R., 1992. Hybridoma perfusion systems: a comparison study. Biotechnol. Bioeng. 40, 25–32.

Ducommun, P., Kadouri, A., von Stockar, U., Marison, I.W., 2002a. On-line determination of animal cell concentration in two industrial high-density culture processes by dielectric spectroscopy. Biotechnol. Bioeng. 77, 316–323.

Ducommun, P., Ruffieux, P., Kadouri, A., von Stockar, U., Marison, I.W., 2002b. Monitoring of temperature effects on animal cell metabolism in a packed bed process. Biotechnol. Bioeng. 77, 838–842.

Gnoth, S., Jenzsch, M., Simutis, R., Lubbert, A., 2007. Process analytical technology (PAT): batch-to-batch reproducibility of fermentation processes by robust process operational design and control. J. Biotechnol. 132, 180–186.

Harris, C.M., Todd, R.W., Bungard, S.J., Lovitt, R.W., Morris, J.G., Kell, D.B., 1987. Dielectric permittivity of microbial suspensions at radio frequencies: a novel method for the real-time estimation of microbial biomass. Enzyme Microb. Technol. 9, 181–186.

Heinrich, C., Beckmann, T., Buntemeyer, H., Noll, T., 2011. Utilization of multifrequency permittivity measurements in addition to biomass monitoring. BMC Proc. 5, O10.

Holland, M., Yagi, H., Takahashi, N., Kato, K., Savage, C.O.S., Goodall, D.M., Jefferis, R., 2006. Differential glycosylation of polyclonal IgG, IgG-Fc and IgG-Fab isolated from the sera of patients with ANCA-associated systemic vasculitis. Bba-Gen. Subjects 1760, 669–677.

Jefferis, R., 2005. Glycosylation of recombinant antibody therapeutics. Biotechnol. Progress 21, 11–16.

Jefferis, R., 2009. Recombinant antibody therapeutics: the impact of glycosylation on mechanisms of action. Trends Pharmacol. Sci. 30, 356–362.

Kaufmann, H., Mazur, X., Fussenegger, M., Bailey, J.E., 1999. Influence of low temperature on productivity, proteome and protein phosphorylation of CHO cells. Biotechnol. Bioeng. 63, 573–582.

Knazek, R.A., Gullino, P.M., Kohler, P.O., Dedrick, R.L., 1972. Cell culture on artificial capillaries: an approach to tissue growth in vitro. Science 178, 65–66.

Kompala, D.S., Ozturk, S.S., 2005. Optimization of high cell density perfusion bioreactors. In: Hu, S.S.O.W.-S. (Ed.), Cell Culture Technology For Pharmaceutical And Cell-Based Therapies. Taylor & Francis.

Langer, E.S., 2011. Trends in perfusion bioreactors. BioProcess Int. 9, 4.

Lee, J.C., Chang, H.N., Oh, D.J., 2005. Recombinant antibody production by perfusion cultures of rCHO cells in a depth filter perfusion system. Biotechnology Progress 21, 134–139.

Looby, D., Griffiths, J.B., 1988. Fixed bed porous glass sphere (porosphere) bioreactors for animal cells. Cytotechnology 1, 339–346.
Markx, G.H., Davey, C.L., Kell, D.B., 1991. To what extent is the magnitude of the cole-cole-alpha of the beta-dielectric dispersion of cell-suspensions explicable in terms of the cell-size distribution. Bioelectrochem. Bioenerg. 25, 195–211.
Meuwly, F., Ruffieux, P.A., Kadouri, A., von Stockar, U., 2007. Packed-bed bioreactors for mammalian cell culture: bioprocess and biomedical applications. Biotechnol. Adv. 25, 45–56.
Mimura, Y., Ashton, P.R., Takahashi, N., Harvey, D.J., Jefferis, R., 2007. Contrasting glycosylation profiles between Fab and Fc of a human IgG protein studied by electrospray ionization mass spectrometry. J. Immunol. Methods 326, 116–126.
Mitsuda, S., Matsuda, Y., Kobayashi, N., Suzuki, A., Itagaki, Y., Kumazawa, E., Higashio, K., Kawanishi, G., 1991. Continuous production of tissue plasminogen-activator (T-Pa) by human embryonic lung diploid fibroblast, Imr-90Cells, using a ceramic bed reactor. Cytotechnology 6, 23–31.
Noll, T., Biselli, M., 1998. Dielectric spectroscopy in the cultivation of suspended and immobilized hybridoma cells. J. Biotechnol. 63, 187–198.
Oh, D.J., Chang, H.N., 1992. High density culture of hybridoma cells in a dual hollow fiber bioreactor. Biotechnol. Tech. 6, 77–82.
Oh, D.J., Choi, S.K., Chang, H.N., 1994. High-density continuous cultures of hybridoma cells in a depth filter perfusion system. Biotechnol. Bioeng. 44, 895–901.
Piret, J.M., Cooney, C.L., 1990. Mammalian-cell and protein distributions in ultrafiltration hollow fiber bioreactors. Biotechnol. Bioeng. 36, 902–910.
Rodriguez, J., Spearman, M., Tharmalingam, T., Sunley, K., Lodewyks, C., Huzel, N., Butler, M., 2010. High productivity of human recombinant beta-interferon from a low-temperature perfusion culture. J. Biotechnol. 150, 509–518.
Rustandi, R.R., Washabaugh, M.W., Wang, Y., 2008. Applications of CE SDS gel in development of biopharmaceutical antibody-based products. Electrophoresis 29, 3612–3620.
Sarra, M., Ison, A.P., Lilly, M.D., 1996. The relationships between biomass concentration, determined by a capacitance-based probe, rheology and morphology of *Saccharopolyspora erythraea* cultures. J. Biotechnol. 51, 157–165.
Tachibana, H., Seki, K., Murakami, H., 1993. Identification of hybrid-type carbohydrate chains on the light-chain of human monoclonal-antibody specific to lung adenocarcinoma. Biochim. Biophys. Acta 1182, 257–263.
Teixeira, A.P., Oliveira, R., Alves, P.M., Carrondo, M.J.T., 2009. Advances in on-line monitoring and control of mammalian cell cultures: supporting the PAT initiative. Biotechnol. Adv. 27, 726–732.
Tharmalingam, T., Sunley, K., Butler, M., 2008. High yields of monomeric recombinant beta-interferon from macroporous microcarrier cultures under hypothermic conditions. Biotechnol. Progress 24, 832–838.
Trummer, E., Fauland, K., Seidinger, S., Schriebl, K., Lattenmayer, C., Kunert, R., Vorauer-Uhl, K., Weik, R., Borth, N., Katinger, H., Muller, D., 2006. Process parameter shifting: part I. Effect of DOT, pH, and temperature on the performance of Epo-Fc expressing CHO cells cultivated in controlled batch bioreactors. Biotechnol. Bioeng. 94, 1033–1044.
Tsai, Y.S., Yoon, S.J., Chuppa, S., Konstantinov, K., Naveh, D., 1996. Fermentor temperature as a tool for control of high-density perfusion cultures of mammalian cells. Abstr. Pap. Am. Chem. Soc. 211, 128-BIOT.
Voisard, D., Meuwly, F., Ruffieux, P.A., Baer, G., Kadouri, A., 2003. Potential of cell retention techniques for large-scale high-density perfusion culture of suspended mammalian cells. Biotechnol. Bioeng. 82, 751–765.
Wang, G., Zhang, W., Jacklin, C., Freedman, D., Eppstein, L., Kadouri, A., 1992. Modified celliGen-packed bed bioreactors for hybridoma cell cultures. Cytotechnology 9, 41–49.
Yoon, S.K., Song, J.Y., Lee, G.M., 2003. Effect of low culture temperature on specific productivity, transcription level, and heterogeneity of erythropoietin in Chinese hamster ovary cells. Biotechnol. Bioeng. 82, 289–298.
Zeiser, A., Bedard, C., Voyer, R., Jardin, B., Tom, R., Kamen, A.A., 1999. On-line monitoring of the progress of infection in Sf-9 insect cell cultures using relative permittivity measurements. Biotechnol. Bioeng. 63, 122–126.
Zhang, Y., Stobbe, P., Orrego Silvander, C., Chotteau, V., 2015. Cell distribution inside the matrix. (Updated in supplementary material).
Zhu, H., Yang, S.T., 2004. Long-term continuous production of monoclonal antibody by hybridoma cells immobilized in a fibrous-bed bioreactor. Cytotechnology 44, 1–14.